Integrated in-band optical signal-to-noise ratio monitor implemented on SOI platform

Lianxi Jia,[1,*] Junfeng Song,[1,2] Tsung-Yang Liow,[1] Qing Fang,[3] Mingbin Yu,[1] G. Q. Lo,[1] and Dim-Lee Kwong[1]

[1]*Institute of Microelectronics, A*STAR (Agency of Science and Technology Research), 11 Science Park Road, Science Park II, 117685 Singapore*

[2]*State Key Laboratory on Integrated opto-electronics, College of Electronic Science and Engineering, Jilin University, Changchun, 130023 China*

[3]*Optoelectronic System Laboratory, Institute of Semiconductors, Chinese Academy of Sciences, Beijing, 100083 China*

[*]*jialx@ime.a-star.edu.sg*

Abstract: Based on different coherence properties of signal and noise, we measured the in-band optical signal-to-noise ratio using an integrated thermally tunable Mach-Zehnder optical delay interferometer on SOI platform. The experimental results exhibit errors smaller than 1 dB for signals with bit rate <40 Gbps over an OSNR range of 9~30 dB. The effects of the extinction ratio, noise equivalent bandwidth and arm length difference on the implementation of measurement are analyzed.

OCIS codes: (130.3120) Integrated optics devices; (060.4510) Optical communications.

References and links

1. D. C. Kilper, R. Bach, D. J. Blumenthal, D. Einstein, T. Landolsi, L. Ostar, M. Preiss, and A. E. Willner, "Optical performance monitoring," J. Lightwave Technol. **22**(1), 294–304 (2004).
2. J. H. Lee, D. K. Jung, C. H. Kim, and Y. C. Chung, "OSNR monitoring technique using polarization-nulling method," IEEE Photon. Technol. Lett. **13**(1), 88–90 (2001).
3. X. Liu, Y.-H. Kao, S. Chandrasekhar, I. Kang, S. Cabot, and L. L. Buhl, "OSNR monitoring method for OOK and DPSK based on optical delay interferometer," IEEE Photon. Technol. Lett. **19**(15), 1172–1174 (2007).
4. E. Flood, W. H. Guo, D. Reid, M. Lynch, A. L. Bradley, L. P. Barry, and J. F. Donegan, "In-band OSNR monitoring using a pair of Michelson fiber interferometers," Opt. Express **18**(4), 3618–3625 (2010).
5. J. Schröder, O. Brasier, T. D. Vo, M. A. F. Roelens, S. Frisken, and B. J. Eggleton, "Simultaneous multi-channel OSNR monitoring with a wavelength selective switch," Opt. Express **18**(21), 22299–22304 (2010).
6. W. Bogaerts, V. Wiaux, P. Dumon, D. Taillaert, J. Wouters, S. Beckx, J. van Campenhout, B. Luyssaert, D. van Thourhout, and R. Baets, "Large-scale production techniques for photonic nanostructures," Proc. SPIE **5335**, 101–112 (2003).
7. K. Yamada, T. Tsuchizawa, T. Watanabe, J. Takahashi, E. Tamechika, M. Takahashi, S. Uchiyama, H. Fukuda, T. Shoji, S. Itabashi, and H. Morita, "Microphotonics devices based on silicon wire waveguiding system," IEICE Trans. Electron," E **87-C**, 351–358 (2004).
8. R. Soref, "The past, present, and future of silicon photonics," IEEE J. Sel. Top. Quantum Electron. **12**(6), 1678–1687 (2006).
9. J. F. Song, H. Zhao, Q. Fang, S. H. Tao, T. Y. Liow, M. B. Yu, G. Q. Lo, and D. L. Kwong, "Effective thermo-optical enhanced cross-ring resonator MZI interleavers on SOI," Opt. Express **16**(26), 21476–21482 (2008).
10. Q. Fang, T. Y. Liow, J. F. Song, K. W. Ang, M. B. Yu, G. Q. Lo, and D. L. Kwong, "WDM multi-channel silicon photonic receiver with 320 Gbps data transmission capability," Opt. Express **18**(5), 5106–5113 (2010).
11. Q. Fang, Y. T. Phang, C. W. Tan, T. Y. Liow, M. B. Yu, G. Q. Lo, and D. L. Kwong, "Multi-channel silicon photonic receiver based on ring-resonators," Opt. Express **18**(13), 13510–13515 (2010).
12. J. F. Song, Q. Fang, S. H. Tao, T. Y. Liow, M. B. Yu, G. Q. Lo, and D. L. Kwong, "Fast and low power Michelson interferometer thermo-optical switch on SOI," Opt. Express **16**(20), 15304–15311 (2008).
13. T. Barwicz, M. R. Watts, M. A. Popovic, P. T. Rakich, L. Socci, F. X. Kartner, E. P. Ippen, and H. I. Smith, "Polarization-transparent microphotonic devices in the strong confinement limit," Nat. Photonics **1**(1), 57–60 (2007).
14. H. Fukuda, K. Yamada, T. Tsuchizawa, T. Watanabe, H. Shinojima, and S. Itabashi, "Silicon photonic circuit with polarization diversity," Opt. Express **16**(7), 4872–4880 (2008).
15. J. Zhang, H. J. Zhang, S. Y. Chen, M. B. Yu, G. Q. Lo, and D. L. Kwong, "A tunable polarization diversity silicon photonics filter," Opt. Express **19**(14), 13063–13072 (2011).

#157708 - $15.00 USD Received 7 Nov 2011; revised 9 Jan 2012; accepted 10 Jan 2012; published 28 Mar 2012

16. J. D. Marconi, S. Arismar Cerqueira, Jr., J. T. Robinson, N. Sherwood-Droz, Y. Okawachi, H. E. Hernandez-Figueroa, M. Lipson, A. L. Gaeta, and H. L. Fragnito, "Performance investigation of microphotonic silicon devices in a field trial all-optical network," Opt. Commun. **282**(5), 849–855 (2009).

1.Introduction

Optical performance monitoring is of key importance for the optical network maintenance and failure diagnosis. Accurate and real-time monitoring of the signal is desired to manage the transparency of the network and locate the failure locations in the network [1]. Optical signal-to-noise ratio (OSNR) is a key performance indicator and monitoring OSNR evolution can provide the vital performance of the network.

In modern optical network, wavelength division multiplexing (WDM) technology is widely utilized. The spectral channels are the fundamental element to be operated and the adjacent channels may experience totally different paths in the network. Thus traditional techniques based on optical spectral measurement are invalid, which determine the in-band OSNR via interpolation from the out-of-band noise level. Several in-band monitoring techniques have been reported based on the different polarization or coherence properties of signal and noise [2–5]. The polarization-nulling method based on the different polarization properties of signal and noise [2] assumes that the signal is fully polarized and the noise is fully un-polarized and distinguishes the signal and noise through through convertion the polarization state of the signal into linear polarization and filtering it with slow changing linear polarizer, which is difficult to realize in the integrated optics. The interferometry method based on the different coherence properties of signal and noise is easy to realize with integrated interferometer and immune to the effects of chromatic dispersion, bit-rate and modulation format [3–5].

The previous devices using interferometry to monitor OSNR are lack of further integration with other optical and electrical devices [3–5]. Silicon photonics has attracted much attention due to its ability to integrate kinds of electronic-photonic components on a single chip [6–11], which significantly simplifies assembly processes and drastically reduces the size and cost of devices.

In this work, we demonstrated, for the first time, the implementation of the OSNR monitoring based on the interferometry on SOI platform. A Mach-Zehnder optical delay interferometer (MZ-ODI) with thermal tunability was fabricated on SOI chip and the OSNR of the non-return-zero on-off-key (NRZ-OOK) signal was measured with ± 1 dB error. The experimental results show good bit-rate-independent property within 40 Gbps, which is valuable for the application of the method in the network. On the basis of current work, further integration with filter and photodetector (PD) on a single chip is expected [10,11], which can realize signal de-multiplexing, performance monitoring and detecting simultaneously.

2. Device operating principle

A signal with high modulation rate remains partially coherent over several bit-periods, while the noise coherence is determined by the channel bandwidth and is significantly shorter than the signal coherence. If the separate coherence of signal and noise is known, it is possible to calculate the OSNR [3]. Here we use MZ-ODI to measure the separate coherence of signal and noise. An optical delay line between the two arms of a MZ is applied as shown in Fig. 1, which generates a time delay to the propagation light in the two arms. When the time delay is long enough, the different coherence of signal and noise can be distinguished. Reference [5] shows that a time delay longer than 2 ps is sufficient in the network. Then, the OSNR can be determined by the following equation [3]:

#157708 - $15.00 USD Received 7 Nov 2011; revised 9 Jan 2012; accepted 10 Jan 2012; published 28 Mar 2012

$$OSNR(dB) = 10\lg\left(\frac{1}{\frac{(n+1)(s-n)}{(R-n)(s+1)} - \frac{n+1}{s+1}} \times \frac{\Delta\nu}{12.5GHz}\right), \quad (1)$$

where $\Delta\nu$ is the noise equivalent bandwidth (NEB), which is usually determined by the effective bandwidth of band-pass filter, n and s are respectively the power ratios of construction over destruction of noise- and signal-only and R is the power ratio of construction over destruction of the total light. In order to get n, s and R, the interference of the MZ-ODI must be tuned to cover the construction and destruction. For realizing this function, a phase shifter is introduced in one arm of the MZ to tune the phase difference between the two arms. In realistic implementation of this method, s can be measured at the input port of the WDM network, which is mainly dependent on the characteristic of the interferometer and the signal spectrum, while n can be determined by running the network without an input signal for a short period. n and s are relatively stable in each node of the network. Thus R is the only parameter to measure for realizing the real-time monitoring of the OSNR.

3. Fabrication and characterization

The MZ-ODI structure is shown in Fig. 1. The waveguides are channel type with typical width 600 nm and height 220 nm. Spot size converters (SSCs) with tip width 180 nm are integrated at the input and output terminals of the device to enhance the coupling efficiency between the waveguide and fiber. A Y-splitter is used to split the input power into the two arms of the interferometer with 50-50 ratio and a same Y-splitter is used to combine the light from the two arms. An extra waveguide is added to one arm as the optical delay line between the two arms. A heater is formed in the other arm as phase shifter to tune the interference of the MZ for measuring n, s and R. These structures were fabricated on an 8-inch SOI wafer with 220 nm top silicon layer and 2 μm buried silica layer. 248-nm deep ultraviolet (UV) photolithography was used to define the pattern of the devices and magnetically-enhanced-reactive-ion-etching process was used to etch the top Si layer. Then, 1.5 μm silica layer was deposited as the separate layer to avoid the metal absorption by plasma enhanced chemical vapor deposition (PECVD). 120 nm titanium Nitride (TiN) was sputtered on the separate layer and a TiN heater was fabricated by UV photolithography and dry etching. 500 nm silica layer was deposited to cover the heater by PECVD. Then, the contact holes to the heater were opened followed by the formation of Al wires and pads. Finally, the end-face of the SSC was exposed by a deep trench etching process as the fiber-to-chip interface.

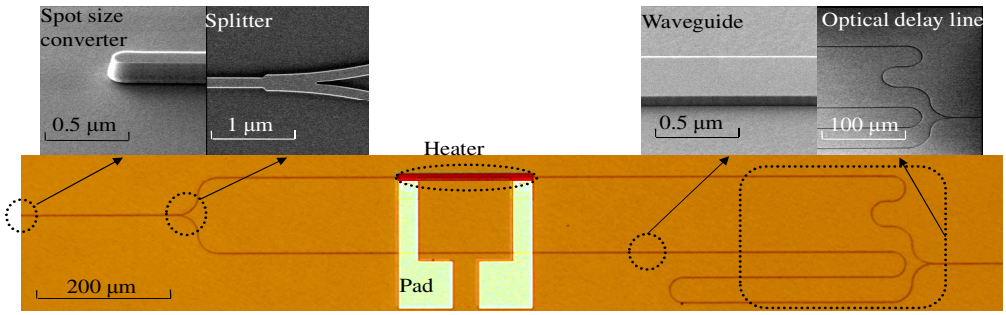

Fig. 1. Mach-Zehnder optical delay interferometer with heater as phase shifter. The arm length difference is 600 μm.

Figure 2 shows the schematic setup of the experiment. The continuous wave output of a tunable laser is modulated by a commercial MZ modulator using the NRZ-OOK electrical

#157708 - $15.00 USD Received 7 Nov 2011; revised 9 Jan 2012; accepted 10 Jan 2012; published 28 Mar 2012

pseudo-random bit sequence of length 2^{31}-1 generated by the pattern generator to produce NRZ-OOK optical signal. An ASE source is used to simulate the noise in the network and the noise level is controlled by a variable optical attenuator (VOA) to change the OSNR. Two polarization controllers (PC) are used to control the separate polarization state of the laser and ASE light source due to the polarization-dependent property of the MZ-ODI on SOI platform. In the experiment we set the polarization states of the both light to quasi-TE mode. The signal and noise are combined together through a tip-coupler. One output port of the coupler is connected to an optical spectrum analyzer (OSA) to get the reference OSNR, another port is connected to a tunable band-pass filter (TBPF) to select the different wavelength channel and change NEB. Then, the filtered light is coupled into the MZ-ODI through a tapered fiber. And the heater is connected to a voltage suppler to generate phase shift with thermal-optical effect. A low-speed PD is used to detect the output optical power of the MZ which will be changed by the phase shift.

We implement this method using the sample with 600 μm arm length difference, which corresponds to ~8 ps time delay and ~1 nm free spectral range (FSR) in the interference spectrum. The signal wavelength is set to 1542.9 nm. The measured extinction ratio of the MZ-ODI at this wavelength is 21.8 dB, which is determined by the uniformity of the Y-splitter and the delay-dependent-loss. The NEB is set to 100 GHz as the ITU grid also centered at 1542.9 nm. Gradually increasing the applied voltage of the phase shifter from 0 V to 4.5 V generates a phase change of 2π with a power consumption of 120 mW and tunes the interference in the output of MZ-ODI over a period, which is necessary for measuring *n*, s and *R*. The response time of the device is limited by the thermal-optic effect, which has the response time in the order of tens of microsecond as shown in our previous work [12]. For ensuring the accuracy of the measurement, we set the voltage step of the scanning to 0.1 V and the time step of the scanning is constrained by the voltage supplier with voltage setting time 6 ms. The total implementation time is about 270 ms.

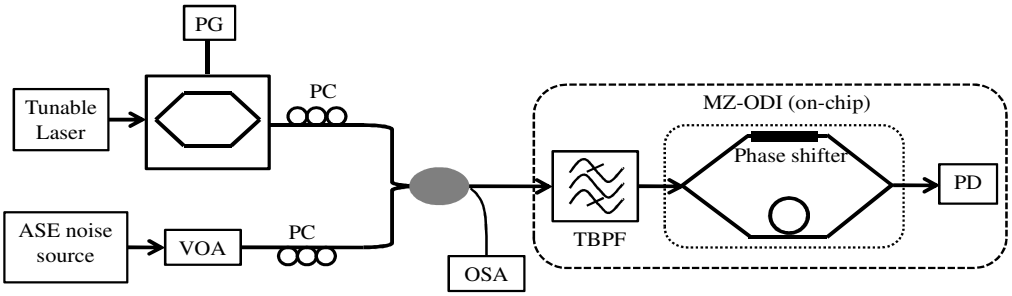

Fig. 2. Schematic of the experimental setup.

Firstly, *n* and *s* are measured with the noise- and signal-only. The measured value of *n* is 1.45 for the fixed 100 GHz filter bandwidth. While the value of *s* changes as the bit-rate of the signal. For the continuous wave (CW) signal, *s* is equal to the ER of the MZ-ODI, which is about 150. As the increase of the bit-rate the signal spectrum is broadened, and the coherence length of the signal is reduced. The measured values of *s* for 10 Gbps and 40 Gbps NRZ-OOK signals are 47 and 16 respectively. The values of *n* and *s* are critical to the measured results of OSNR, so repeated calibration is needed to ensure the proper reading.

Then, *R* is obtained with both noise and signal on. The VOA is used to change the OSNR and the measured *R* as a function of OSNR is shown in Fig. 3(a). The value of *R* should be in the interval of (*n*, *s*), which is verified by all the measured results. Then, the OSNRs can be calculated according Eq. (1) as shown in Fig. 3(b) as a function of the reference OSNR. The results exhibit good uniformity for the three signals with different bit-rate over an OSNR range of 9~30 dB with errors all within ± 1 dB.

Although the results show good independence on the bit-rate, the bit-rate affects the measurement tolerance of *R*, which is mainly caused by the different *s* value. The slope of the

#157708 - $15.00 USD Received 7 Nov 2011; revised 9 Jan 2012; accepted 10 Jan 2012; published 28 Mar 2012

solid curves in Fig. 3(a), which are the calculated value of R for different OSNR according Eq. (1) with measured s and n, reflects the measurement tolerance of R. It is clearly shown that the increase of s can increase the slope of the curves, which corresponds to the enhancement of measurement tolerance of R especially for the high OSNR. So a large s is preferred for the implementation of this method.

s is determined by the ER of the interferometer except for the bit-rate. For fixed bit-rate, the value of s is proportional to ER. A MZ-ODI with large ER can extend the measurement tolerance so as to further enlarge the measurement range for bit-rate. In our experiment a sample with best ER was selected. Other samples with bad ER were also tested and the performance for measuring high OSNR signal was poor restricted by the small s value. Although large ER also increase the value of n, it is neglectable compared to the increase of s. Higher ER can be realized by a directional coupler in place of the Y-splitter [12].

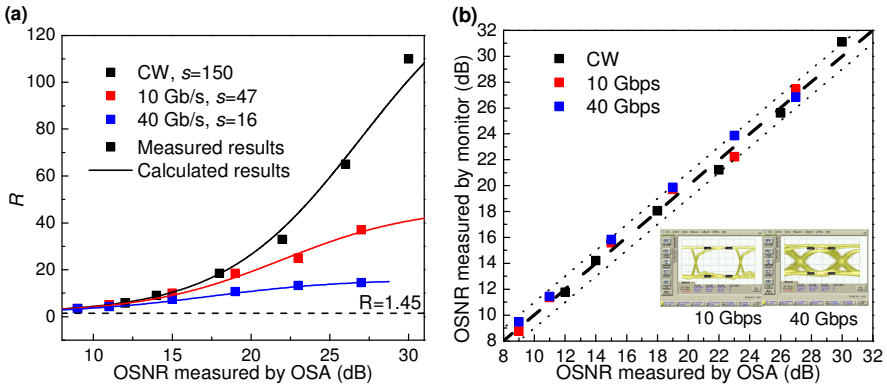

Fig. 3. (a) The measured R (scatters) as a function of reference OSNR for NRZ-OOK signals with different bit-rate and the calculated R (solid lines). (b) OSNR measurement as a function of reference OSNR. Insets are the eye diagrams of the input signals with 10 Gbps and 40 Gbps bit-rate. Dotted lines represent the errors of ± 1 dB.

NEB is another factor that affects the measurement, which can easily be tuned by changing the bandwidth of the TBPF. As shown in Fig. 4(a), when the NEB is decreased to 175 GHz from 350 GHz, the noise coherence will increase shown as the increase of n from 1.1 to 1.36. The noise power is also reduced shown as the increase of the measured R for each OSNR. The value of s is almost unaffected by NEB and the measured OSNRs are all within ± 1 dB error as shown in Fig. 4(b). The selection of NEB is mainly determined by the channel spacing of the network and the spectrum of the signal.

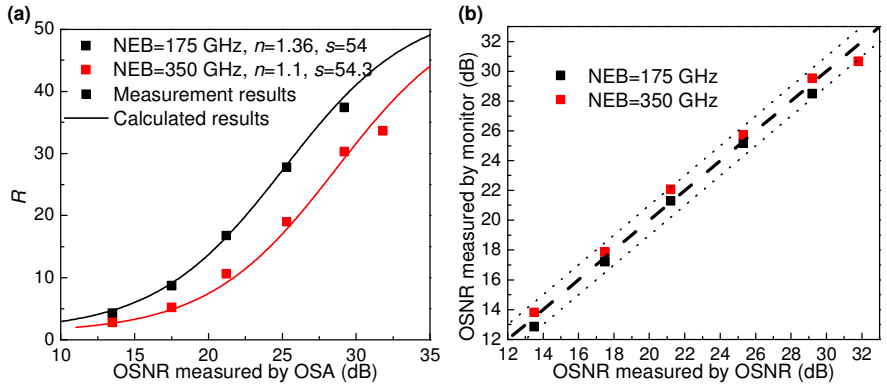

Fig. 4. (a) The measured R (scatters) as a function of reference OSNR for different NEB and the calculated R (solid lines). (b) OSNR measurement as a function of reference OSNR. Dotted lines represent the errors of ± 1 dB.

#157708 - $15.00 USD Received 7 Nov 2011; revised 9 Jan 2012; accepted 10 Jan 2012; published 28 Mar 2012

We also analyzed the effect of arm length difference of the MZ-ODI on the measurement. Two samples with arm length difference of 600 μm and 900 μm were tested. As the increase of the arm length difference, the time delay and delay-dependent-loss both increase, which reduce the ER of the interferometer and the coherence of signal and noise. In the measurement we set the NEB to 100 GHz. The measured n and s are respectively 1.2 and 110 for device with 900 μm arm length difference when the signal is CW signal, which have small reduction compared to device with 600 μm arm length difference. The measured results are shown in Fig. 5. Little difference exists caused by the different ER. If the time delay is sufficiently large as declared in reference 5 and the ER is not much reduced by the increase of arm length difference, the effect of the arm length difference is almost negligible.

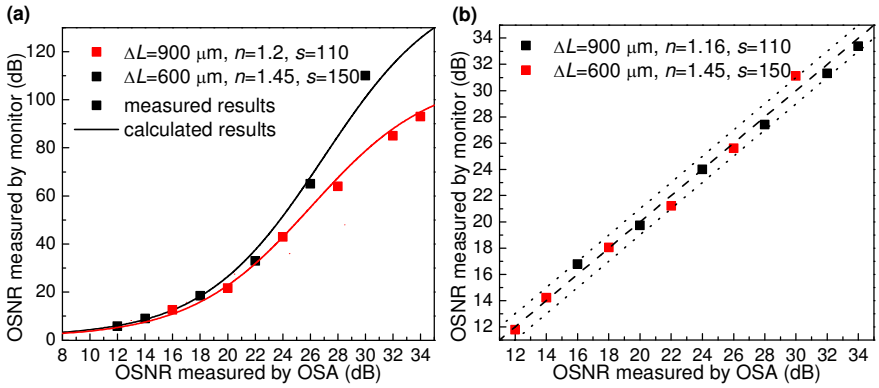

Fig. 5. (a) The measured *R* (scatters) as a function of reference OSNR for samples with different arm length difference and the calculated *R* (solid lines). (b) OSNR measurement as a function of reference OSNR. Dotted lines represent the error of ± 1 dB

4. Summary and discussion

We realized in-band OSNR monitoring with MZ-ODI on SOI platform, covering an OSNR range of 9~30 dB with ± 1 dB error. The measurement results show good bit-rate-independent property. The effects of the extinction ratio, NEB and arm length difference on the measurement are analyzed. The present devices are still polarization dependent, which will limit its application in the network. Polarization diversity scheme can be used to overcome this obstacle [13–15] and dynamic polarization controller can be another alternative, which can convert the random polarization state of the light from the network to the required polarization state as shown in reference 16. In the future work, we will try to integrate the tunable filter and PD with the MZ-ODI, as shown in the dashed square in Fig. 2, on a single chip. Thus, on-chip optical signal performance monitoring can be achieved without the assistant of off-chip devices.

#157708 - $15.00 USD Received 7 Nov 2011; revised 9 Jan 2012; accepted 10 Jan 2012; published 28 Mar 2012